

ARTICLE TYPE

Real-time Segmentation and Facial Skin Tones Grading[†]

Ling Luo^{*1} | Dingyu Xue¹ | Xinglong Feng¹ | Yichun Yu² | Peng Wang³¹Northeastern University, Shenyang, China²Beihang University, Beijing, China³Microsoft Research Asia, Beijing, China**Correspondence**

*Ling Luo, Northeastern University. Email: lingluo@stu.neu.edu.cn

Present Address

Meidaojia, Beijing, China

Summary

Modern approaches for semantic segmentation usually pay too much attention to the accuracy of the model, and therefore it is strongly recommended to introduce cumbersome backbones, which brings heavy computation burden and memory footprint. To alleviate this problem, we propose an efficient segmentation method based on deep convolutional neural networks (DCNNs) for the task of hair and facial skin segmentation, which achieving remarkable trade-off between speed and performance on three benchmark datasets. As far as we know, the accuracy of skin tones classification is usually unsatisfactory due to the influence of external environmental factors such as illumination and background noise. Therefore, we use the segmented face to obtain a specific face area, and further exploit the color moment algorithm to extract its color features. Specifically, for a 224×224 standard input, using our high-resolution spatial detail information and low-resolution contextual information fusion network (HLNet), we achieve **90.73%** Pixel Accuracy on Figaro1k dataset at over **16 FPS** in the case of CPU environment. Additional experiments on CamVid dataset further confirm the universality of the proposed model. We further use masked color moment for skin tones grade evaluation and approximate **80%** classification accuracy demonstrate the feasibility of the proposed scheme. Code is available at <https://github.com/JACKYLUO1991/Face-skin-hair-segmentaiton-and-skin-color-evaluation>.

KEYWORDS:

hair and skin segmentation, deep convolutional neural network, skin tones classification, color moment

arXiv:1912.12888v2 [cs.CV] 9 Jan 2020

1 | INTRODUCTION

AR (Augmented Reality) technology has become a hot spot recently due to its widespread application in various domains, and the most widely used is the beauty industry. Among them, automatic hair dyeing (in Fig. 1) is one of the major applications in the beauty industry. However, there are enormous challenges in the actual application scenario. First of all, because the hair has a very complex shape structure¹, it is quite difficult to handle accurate edge information. Although the existing semantic segmentation methods^{2,3,4} have relatively high segmentation performance for simple objects, only a relatively rough mask can be obtained in the processing of hair segmentation task. Secondly, almost all networks require GPU with high computation power that most of mobile devices do not have. It greatly limits the using scenario. Thirdly, taking into account runtime limitations, Conditional Markov random fields (CRFs)⁵ is not suitable for edge processing. Taking all these factors into considerations, real-time hair dyeing faces enormous challenges. At the same time, e-commerce and digital interaction with the clients allows people to buy their favorite products without leaving home. Among them, the robust product recommendation function plays an

[†]Part of this work was done when L. Luo was an intern at Meidaojia, Beijing, China.

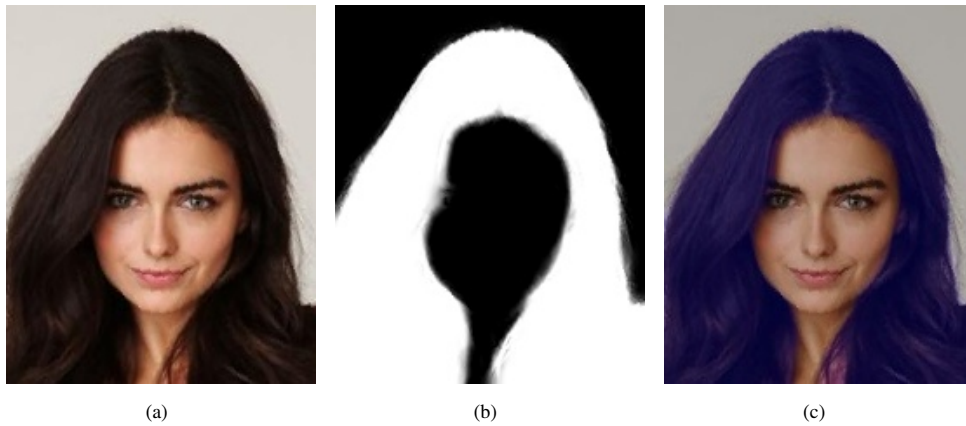


FIGURE 1 Automatic hair dyeing exemplar. (a) Input RGB image. (b) The guided filter output of our proposed algorithm. (c) Final dyed rendering.

important role. Automatic assessment of skin tones levels which makes it possible to personalize recommendation for beauty products. However, in the context of a complex environment, skin tones grading is influenced by lighting, shadows, and imaging equipment etc. that even an experienced skin therapist is difficult to judge with the naked eye. This paper is dedicated to solving these problems using machine learning and fiery deep learning algorithms.

Semantic segmentation is an advanced visual task, whose goal is to assign different category labels to each pixel. However, limited by bulky backbones, existing state-of-the-art models are not suitable for actual deployment. In this paper, we strive to balance the relationship between the efficiency and speed of segmentation network, and provide a much simpler and more compact alternative for our multi-task segmentation scenario. In order to get accurate segmentation results, global information and context information should be considered simultaneously. Based on this observation, we propose a spatial and context information fusion framework (HLNet) that high-dimensional and low-dimensional feature maps are integrated into one network. Further experiments confirm that HLNet achieve significant trade-off between efficiency and accuracy. Considering that background illumination is not conducive to identifying skin tones, we extract features (*a.k.a.* masked color moments) based on the segmented face and color moment algorithm. After that, the mask color moments are input into a powerful Random Forest Classifier to evaluate a person's skin tone level.

The remainder of the paper is organized as follows. In Section 2, we briefly review the latest real-time and efficient deep-learning based semantic segmentation proposals as well as domain-specific segmentation algorithms in the field of computer vision. We elaborate on the process of our scheme in Section 3, then ablation and contrast experiments are performed in Section 4. At last, we summarize our work and future research directions in Section 5.

2 | RELATED WORK

2.1 | Lightweight model

Since pioneering work² based on deep learning, many high-quality backbones⁶⁷⁸⁹ have been derived. However, due to the requirements of computationally limited platforms (e.g., drones, autonomous driving, smartphone), people pay more attention to the efficiency of the network than just the performance.

*ENet*¹⁰ is the first lightweight network for real-time scene segmentation which does not apply any post-processing steps in an end-to-end manner. Zhao *et al.*¹¹ introduces a cascade feature fusion unit to quickly achieve high-quality segmentation. Howard *et al.*¹² present a compact encoder module which based on a streamlined architecture that uses Depthwise separable convolutions to build light-weight deep neural networks. Poudel *et al.*¹³ combine spatial detail at high resolution with deep features extracted at lower resolution yielding beyond real-time effects. Recently, *LEDNet*¹⁴ has been proposed which channel split and shuffle are utilized in each residual block to greatly reduce computation cost while maintaining higher segmentation accuracy.

2.2 | Contextual information

Some details cannot be recovered during conventional up-sampling of the feature maps to restore the original image size. The design of *skip connections*¹⁵ can alleviate this deficiency to some extent. Zhao *et al.*⁸ propose a pyramid pooling module that can aggregate context information from different regions to improve the ability to capture multi-scale information. Zhang *et al.*¹⁶ design a context encoding module to introduce global contextual information, which is used to capture the context semantics of the scene and selectively highlight the feature map associated with a particular category. Fu *et al.*¹⁷ address the scene parsing task by capturing rich contextual dependencies based on spatial and channel attention mechanisms, which significantly improve the performance on numerous challenging datasets.

2.3 | Post processing

Generally, the quality of the above segmentation methods is obviously rough and requires additional post-processing operations. Post-processing mechanisms are usually able to improve image edge detail and texture fidelity, while maintaining a high degree of consistency with global information. Chen *et al.*¹⁸ propose a CRF post processing method that overcome poor localization in a non-end-to-end way. *CRFasRNN*⁵ considers the CRF iterative reasoning process as an RNN operation in an end-to-end manner. In order to eliminate the excessive execution time of CRF, Levinshtein *et al.*¹⁹ present a hair matting method with real-time performance on mobile devices

2.4 | Color feature extraction

*Color Histograms*²⁰ are widely used color features in many image retrieval systems which describe the proportion of different colors in the entire image. Calculating the color histogram requires dividing the color space into a number of small color intervals, each called a bin. This process is often referred to as color quantization. Since the color space such as HSV and LAB is more in line with people's subjective judgment on color similarity, RGB space is not generally used. The biggest disadvantage of this method is that it cannot represent the local distribution of colors in the image and the spatial location of each color.

*Color Moment*²¹ proposed by Stricker and Orengo is another straightforward and effective color feature. The mathematical basis of this method is that any color distribution in an image can be represented by its moment. In addition, since the color distribution information is mainly concentrated in the low-order moment, only the first moment (mean), the second-order moment (variance) and third-order moment (skewness) of the color are sufficient to express the color distribution of the image. Another benefit of this approach is that it does not require vectorization of features compared to color histograms.

The *Color Correlogram*²² is also an expression of the color distribution of the images. This feature not only depicts the proportion of pixels in a certain color to the entire image, but also reflects the spatial correlation between pairs of different colors. However, this solution is too complicated in time.

Overall, our approach is closely related to asymmetric encoding and decoding structure. Furthermore, we simply employ masked color moment to sort the skin tones, which will be discussed in the next chapter.

3 | METHODOLOGY

In this section, we will elaborate the proposed method and the model framework for hair and face segmentation, as well as the methodological basis for subsequent facial skin tones classification.

3.1 | High-to-low dimension fusion network

The proposed HLNet network is inspired by *HRNet*²³ which maintains high-resolution representation through the whole process by connecting high-to-low resolution convolutions in parallel. Figure 2 illustrates the overall framework of our model. We experimentally prune the model parameters to increase the speed without excessive performance degradation. Furthermore, the existing state-of-the-art modules^{13 24 25 26} are reasonably combined to further improve the performance of the network.

Architecture. Table 1 gives an overall description of the modules involved in the network. The model consists of different kinds of convolution modules, up-sampling (**complementary**: transposed convolution layer can cause gridding artifacts), bottlenecks, and other feature maps communication modules. In the following part, we will expand the above modules in detail.

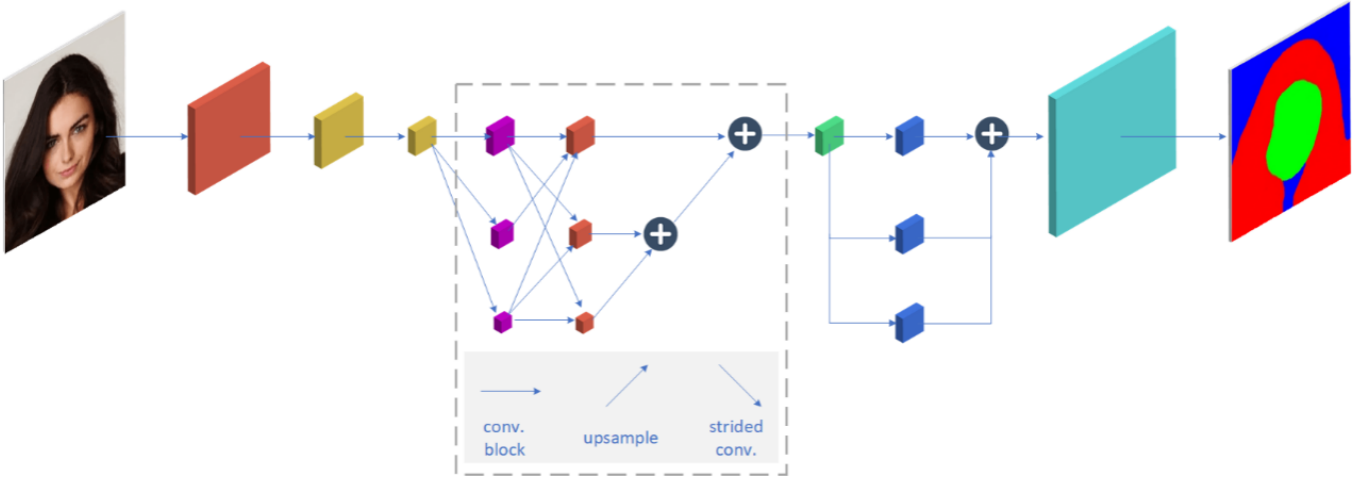


FIGURE 2 An overview of our asymmetric encoder-decoder network. Blue, red and green represents background, hair mask recolored and face mask recolored, respectively. In the dotted rectangle (also called *InteractionModule*), different arrows represent different operations. ‘+’ means *Add* operation.

In the first three layers, we refer to *Fast-SCNN*¹³ to employ standard convolution and depth separable convolution for fast down-sampling in order to ensure low-level feature sharing. Depth separable convolution reduces the amount of model parameters effectively while achieving a comparable representation ability. The above convolution unified use stride 2 and 3×3 spatial kernel size, followed by BN²⁷ and RELU activation function. According to *FCOS*²⁸, the low-dimensional detail information of the feature map promotes the segmentation of small objects, so we superimpose the low-dimensional layers to enhance detail representation ability of the proposed model. Interaction of high-resolution and low-resolution information facilitates learning of multi-level information representation. In this part, we draw the above advantages and propose a information interaction module (*InteractionModule*) with feature maps of different resolutions to obtain elegant output results. Different feature map scales use 1×1 convolution and Bilinear up-sampling module for channel combination and exchange. Up-sampling is characterized by the fact that no weight parameters need to be learned, so we discard the operation of transposed convolution to save computing resources. In addition to standard convolution modules, we also use the efficient inverted bottleneck residual block modules proposed by *MobileNet v2*²⁴ which is illustrated in Figure 3. Subsequently, we followed the *FFM Attention*²⁵ to focus the model on the channel features with the most information and suppress those channel features that are not important. To capture multi-scale context information, we also introduce a multi-receptive field fusion block (*e.g.* dilation rate is set to 2, 4, 8).

For simplicity, the decoder directly performs bilinear upsampling on the 28×28 feature map (**Complementary**: transposed convolution layer can cause gridding artifacts¹⁹), and additionally adds a *SOFTMAX* layer for pixel-wise classification.

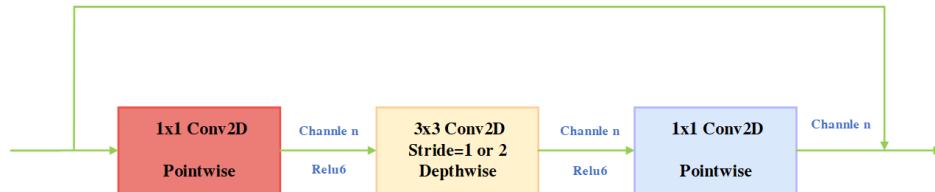


FIGURE 3 Inverted residual module proposed by *MobileNet v2* release. If the stride size is equal to 1, additional shortcut operation is required. In general, $t=6$ enables the separation convolution to extract features in a higher dimension, which effectively improves the representation ability of the model.

Post Processing. In pursuit of perceptual consistency and reduce the time complexity of running, we advocate the idea of *Guided Filter*^{29,30} to achieve edge-preserving and denoising. *Guided Filter* can effectively suppress gradient-reversal artifacts and produce visually pleasing edge profiles. Given a guidance image I and filtering input image P , our goal is to learn a local

linear model to describe the relationship between the former and the output image Q while seeking consistency between P and Q just like the role of *Image Matting*³¹ For simplicity and efficiency, s, r, ζ are set to 4, 4, and 50, respectively, during the experiment.

3.2 | Facial skin tones classification

The second stage is to classify facial skin tones. Usually for Asians, we divide it into *porcelain white, ivory white, medium, yellowish* and *black*. For skin tones features, it is not wise to use deep learning for feature extraction due to its feature space is relatively small, which is easy to cause under-fitting. Therefore, after repeated thoughts and experimental trial and error, the scheme is selected to extract the color moment of the image as the features to be learned and put it into the classic machine learning algorithm for learning. Considering facial skin tones in complex scenes, background lighting has a incurable impact on the results. So we employ image morphology algorithms and pixel-level operations to get rid of background interference. Ultimately, the remaining face regions are used to extract the color moment features and then fed into the machine learning algorithm for learning. As far as the classifier is concerned, we choose the *Random Forest Classifier*³² due to its powerful classification ability. The detail of algorithm is summarized in **Algorithm 1**.

Algorithm 1 : Framework of facial region extraction.

Input: Original rgb image I_i , total number of images N .

Output: Smooth facial region F_i after image processing.

Initial stage: Get the segmentation mask $M_i^c (c \subseteq 0, 1, 2)$ with the help of our *HLNet*.

for each $i \in N$ **do**

Extract rough facial mask region M_i^2 (For the convenience of description, it is referred to as M_i),

Referring to *Image Erode Formula* **dst** $P_i(x, y) \leftarrow \min \text{src } M_i(x + x', y + y')$ **where** $\text{element}(x', y') \neq 0$ in order to eliminate mask gaps,

Use *Bilateral Filtering* to smooth mask edges, as Q_i ,

The final F_i is obtained by *Bitwise and* operation between I_i and Q_i .

end for

4 | EXPERIMENTAL EVALUATION

we evaluate the segmentation performance of hair and skin segmentation on three public datasets and further confirm the generalization of the proposed architecture on the challenging benchmark vehicle road dataset *CamVid*³³. In the following, we begin with a brief introduction to the datasets which involved in the experiment, including a manually annotated dataset. Next, by comparing with the existing scheme and conducting ablation experiment, it is proved that our scheme could achieve outstanding trade-off between speed and accuracy. All the networks mentioned below follow the same training strategy, except for the initial learning rate setting. They are trained using mini-batch stochastic gradient descent (SGD) with batch size 64, momentum 0.98 and weight decay $2e-5$ for face-related segmentation datasets. For *CamVid* experiment, we use Adam gradient descent strategy with learning rate $1e-3$ because we found it more conducive to the convergence of the model. The former adopts ‘poly’ learning rate policy in configuration where the initial rate is multiplied by $(1 - \frac{\text{iter}}{\text{total_iter}})^{\text{power}}$ with power 0.9 and initial learning rate is set as $2.5e-3$. In terms of loss function, we apply *generalized dice loss*³⁴ to compensate for the segmentation performance of small objects. Data augmentation includes normalization, random rotation $[-20, 20]$, random scale $[-20, 20]$, random horizontal flip and random shift $[-10, 10]$. For fair comparison, all the methods are conducted on a server equipped with a single NVIDIA GeForce GTX1080Ti GPU.

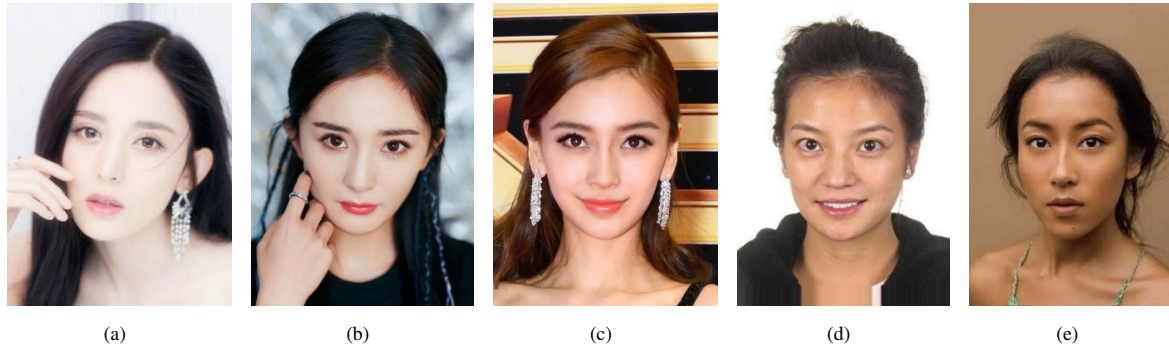


FIGURE 4 Manually marked face skin hue level sample after voting mechanism. From left to right, it represents porcelain white, ivory white, medium, yellowish and black. In order to have a consistent understanding of image classification criteria, only actresses are used here.

4.1 | Database introduction

Data is the soul of deep learning, because it determines the upper limit of an algorithm to some extent. In order to ensure the robustness of the algorithm, it is necessary to construct a dataset with human faces in extreme situation such as large angles, strong occlusions, complex lighting changes etc.

4.1.1 | Face and hair segmentation datasets

*Labeled Faces in the wild (LFW)*³⁵ dataset consists of more than 13,000 images on the Internet. We use its extension version (Part Labels) during the experiment which automatically labeled via a super-pixel segmentation algorithm. We adopt the same data partitioning method in³⁶ as 1500 images in the training, 500 used in validation, and 927 used for testing.

*Large-scale CelebFaces Attributes dataset (CelebA)*³⁷ consisting of more than 200k celebrity images, each with multiple attributes. The main advantage of this dataset is that it combines large pose variations and background clutter making the knowledge learned from this dataset easier to satisfy demand of actual products. In the experiment we adopted the version of CelebA dataset in³⁶ which includes 3556 images. We used the same configuration parameters as the original paper, that is, 20% for validation.

The last dataset of the experiment, we employ *Figaro1k*³⁸ dedicated to hair analysis. However, as this dataset was developed for general hair detection, face is not included in many images. In this case, we apply a universal face detector as¹, which was proposed by the literature. Since only the image of the detected face can participate in subsequent segmentation tasks, 171 images are used for experiments.

4.1.2 | Benchmark CamVid dataset

In order to demonstrate the generalization ability of the proposed method, we also conduct experiments on benchmark CamVid dataset. *CamVid* dataset contains images extracted from video sequences with resolution up to 960×720 . In this experiment, we adopt the same setting as³⁹ which contains 701 images in total, in which 367 for training, 101 for validation and 233 for testing.

4.1.3 | Annotated dataset

One contribution of this work is a manually labeled face skin tones grading dataset. According to different facial tones hue levels of Asians, it is mainly divided into five categories: porcelain white, ivory white, medium, yellowish and black. In the process of labeling, three professionally trained makeup artists rated the face tones color using a voting mechanism. Our face data is also derived from the Internet, leaving only data that contains faces. These data are in turn used for later feature extraction and machine learning. The number of each category is 95, 95, 96, 93 and 94, samples are shown in Figure 4.

4.2 | Segmentation results

In the testing phase, we first use the existing *MTCNN*⁴⁰ with high recall rate to extract the face ROI. Secondly, considering the redundant environmental information has a certain promotion effect on the segmentation background, the ROI region is enlarged with a factor of 0.8 in both horizontal and vertical dimensions. For quantitative evaluation, we use four *FCN*² derived metrics to evaluate the performance of hair and face segmentation algorithms. Table 2 shows the comparison results between our method and the methods in literature.³⁶

One drawback of fast downsampling is that the feature extraction for the shallow layer is not sufficient, so our HLNet is slightly worse than VGG-like networks in CelebA dataset (CelebA facial details are significantly clearer than LFW). However, considering the running time, we reach 63 ms per image in the CPU terminal without any tricks. We can further reach no more than 5 ms under GPU. Comparing VGG with HLNet (64 ms vs 4.7±0.2 ms) shows that the latter is more efficient, while performance is comparable. This conclusion suggests that we can further apply this framework to the edge and embedded devices with small memory and battery budget. The qualitative analysis results are shown in Figure 5. The post-processing employs *Guided Filter* to achieve more realistic edge effects.

Ablation Study We conduct the ablation experiments on Figaro1k test dataset, and follow the same training strategy for the fairness of the experiments. We mainly evaluate the impact of InteractionModule (IM) and DilatedGroup (DG) components on the results, as shown in Table 3. Three parallel 3×3 convolutions and convolutions with a rate of 1 are used to replace the corresponding components as *baseline*. When we append DG and IM modules respectively, mIoU increases by 1.54% and 3.19% relative to the *baseline*. When we apply two modules at the same time, mIoU increases dramatically by 4.26%. The obvious performance gains illustrate the efficiency of the proposed model.

We also give a comparison of our method with the existing methods on the CamVid dataset. We adopt widely used mean-interesection-over-union (mIoU) to evaluate segmentation quality. The results are reported in Table 4. Our HLNet get much faster inference speed while achieving comparable performance compared to the state-of-the-art models.

4.3 | Facial skin tones classification results

In the second phase of the experiment, we use ablation study to compare the influence of different color spaces and different experimental protocols on the results.

In Table 5, we report the facial skin tones classification accuracy. The best results are obtained using the YCrCb space with color moment backend. It should be noted that before the experiment, the data is first oversampled to ensure that the imbalance between the categories is eliminated. We simply split the dataset into 8:2 for training and testing, and then use the powerful Random forest classifier for training. Figure 6 gives the confusion matrix for this configuration. It can be observed from the figure that the main mistakes are between adjacent categories, and this situation also plagues a trained professional makeup artist when he or she labels data.

5 | CONCLUSION

In this paper, we propose a fully convolutional network to solve the real-time segmantic segmentation problem, so as to achieve a trade-off between speed and performance. Through comparative experiments and cross-dataset evaluation, we prove the feasibility and generalization of our method. Next, we propose a method for extracting skin tones features, which extracts masked facial tones features and throws them into a random forest classifier for classification. 80% classification accuracy demonstrate the effectiveness of the proposed solution.

The purpose of this work is to apply our algorithm to real-time dyeing, face swap, skin tones rating system, and skin care product recommendation based on skin tones levels in realistic scenarios. As a future work, we plan to further explore color features to improve classification accuracy.

ACKNOWLEDGMENTS

This work has been supported by the Project of the National Natural Science Foundation of China No.61773104.

Conflict of interest

No potential conflict of interests.

References

1. Muhammad UR, Svanera M, Leonardi R, and Benini S. Hair detection, segmentation, and hairstyle classification in the wild. *Image and Vision Computing*. 2018;**71**:25–37.
2. Long J, Shelhamer E, and Darrell T. Fully convolutional networks for semantic segmentation. *IEEE Transactions on Pattern Analysis & Machine Intelligence*. 2014;**39**(4):640–651.
3. Ronneberger O, Fischer P, and Brox T. U-net: Convolutional networks for biomedical image segmentation. MICCAI 234–141. 18th MICCAI Medical Image Computing and Computer-Assisted Intervention Conference. Munich; October 5–9, 2015. .
4. Yu F, and Koltun V. Multi-scale context aggregation by dilated convolutions. <https://arxiv.org/abs/1511.07122>, arxiv. Accessed April 30, 2016; 2015.
5. Zheng S, Jayasumana S, Romera-Paredes B, Vineet V, Su Z, Du D, et al. Conditional random fields as recurrent neural networks. ICCV 1529-1537. ICCV IEEE International Conference on Computer Vision. Santiago; December 7–13, 2015. .
6. Chen LC, Papandreou G, Schroff F, and Adam H. Rethinking atrous convolution for semantic image segmentation. <https://arxiv.xilesou.top/abs/1706.05587>, arxiv. Accessed December 5, 2017; 2017.
7. Jégou S, Drozdal M, Vazquez D, Romero A, and Bengio Y. The one hundred layers tiramisu: Fully convolutional densenets for semantic segmentation. CVPR Workshops 11-19. CVPRW IEEE Conference on Computer Vision and Pattern Recognition (CVPR) Workshops. Hawaii; July 21–26, 2017. .
8. Zhao H, Shi J, Qi X, Wang X, and Jia J. Pyramid scene parsing network. CVPR 2881-2890. CVPR IEEE Conference on Computer Vision and Pattern Recognition. Hawaii; July 21–26, 2017. .
9. Lin G, Milan A, Shen C, and Reid I. Refinenet: Multi-path refinement networks for high-resolution semantic segmentation. CVPR 1925-1934. CVPR IEEE Conference on Computer Vision and Pattern Recognition. Hawaii; July 21–26, 2017. .
10. Paszke A, Chaurasia A, Kim S, and Culurciello E. Enet: A deep neural network architecture for real-time semantic segmentation. <https://arxiv.xilesou.top/abs/1606.02147>, arxiv. Accessed June 7, 2016; 2016.
11. Zhao H, Qi X, Shen X, Shi J, and Jia J. Icnets for real-time semantic segmentation on high-resolution images. ECCV 405-420. ECCV European Conference on Computer Vision. Munich; September 8–14, 2018. .
12. Howard AG, Zhu M, Chen B, Kalenichenko D, Wang W, Weyand T, et al.. Mobilenets: Efficient convolutional neural networks for mobile vision applications. <https://arxiv.xilesou.top/abs/1704.04861>, arxiv. Accessed April 17, 2017; 2017.
13. Poudel RP, Liwicki S, and Cipolla R. Fast-SCNN: fast semantic segmentation network. <https://arxiv.xilesou.top/abs/1902.04502>, arxiv. Accessed February 12, 2019; 2019.
14. Wang Y, Zhou Q, Liu J, Xiong J, Gao G, Wu X, et al.. LEDNet: A Lightweight Encoder-Decoder Network for Real-Time Semantic Segmentation. <https://arxiv.xilesou.top/abs/1905.02423>, arxiv. Accessed May 13, 2019; 2019.
15. He K, Zhang X, Ren S, and Sun J. Deep residual learning for image recognition. CVPR 770-778. CVPR IEEE Conference on Computer Vision and Pattern Recognition. Las Vegas; June 26–July 1, 2016. .
16. Zhang H, Dana K, Shi J, Zhang Z, Wang X, Tyagi A, et al. Context encoding for semantic segmentation. CVPR 7151-7160. CVPR IEEE Conference on Computer Vision and Pattern Recognition. Salt Lake City; June 19–21, 2018. .
17. Fu J, Liu J, Tian H, Li Y, Bao Y, Fang Z, et al. Dual attention network for scene segmentation. CVPR 3146-3154. CVPR IEEE Conference on Computer Vision and Pattern Recognition. Los Angeles; June 16–20, 2019. .

18. Chen LC, Papandreou G, Kokkinos I, Murphy K, and Yuille AL. Semantic image segmentation with deep convolutional nets and fully connected crfs. <https://arxiv.xilesou.top/abs/1412.7062>, arxiv. Accessed June 7, 2016; 2014.
19. Levinshtein A, Chang C, Phung E, Kezele I, Guo W, and Aarabi P. Real-time deep hair matting on mobile devices. CRV 1-7. 15th CRV Conference on Computer and Robot Vision. Toronto; May 8–10, 2018. .
20. Swain MJ, and Ballard DH. Color indexing. *International Journal of Computer Vision*. 1991;7(1):11–32.
21. Stricker MA, and Orengo M. Similarity of color images. SPIE 381-392. SPIE Symposium on Electronic Imaging. San Jose, CA; March 23, 1995. .
22. Huang J, Kumar SR, Mitra M, Zhu WJ, and Zabih R. Image indexing using color correlograms. CVPR 762-768. CVPR IEEE Computer Society Conference on Computer Vision and Pattern Recognition. San Juan, Puerto Rico; June 17–19, 1997. .
23. Sun K, Xiao B, Liu D, and Wang J. Deep high-resolution representation learning for human pose estimation. <https://arxiv.xilesou.top/abs/1902.09212>, arxiv. Accessed February 25, 2019; 2019.
24. Sandler M, Howard A, Zhu M, Zhmoginov A, and Chen LC. Mobilenetv2: Inverted residuals and linear bottlenecks. CVPR 4510-4520. CVPR IEEE Conference on Computer Vision and Pattern Recognition. Salt Lake City; June 19–21, 2018. .
25. Yu C, Wang J, Peng C, Gao C, Yu G, and Sang N. Bisenet: Bilateral segmentation network for real-time semantic segmentation. ECCV 325-341. ECCV European Conference on Computer Vision. Munich; September 8–14, 2018. .
26. Chollet F. Xception: Deep learning with depthwise separable convolutions. CVPR 1251-1258. CVPR IEEE Conference on Computer Vision and Pattern Recognition. Hawaii; July 21–26, 2017. .
27. Ioffe S, and Szegedy C. Batch normalization: Accelerating deep network training by reducing internal covariate shift. <https://arxiv.xilesou.top/abs/1502.03167>, arxiv. Accessed March 2, 2015; 2015.
28. Tian Z, Shen C, Chen H, and He T. FCOS: Fully Convolutional One-Stage Object Detection. <https://arxiv.xilesou.top/abs/1904.01355>, arxiv. Accessed August 20, 2019; 2019.
29. He K, Sun J, and Tang X. Guided image filtering. ECCV 1-14. 11th ECCV European Conference on Computer Vision. Crete; September 5–11, 2010. .
30. He K, and Sun J. Fast guided filter. <https://arxiv.xilesou.top/abs/1505.00996>, arxiv. Accessed May 5, 2015; 2015.
31. Levin A, Lischinski D, and Weiss Y. A closed-form solution to natural image matting. *IEEE Transactions on Pattern Analysis and Machine Intelligence*. 2007;30(2):228–242.
32. Pal M. Random forest classifier for remote sensing classification. *International Journal of Remote Sensing*. 2005;26(1):217–222.
33. Brostow GJ, Shotton J, Fauqueur J, and Cipolla R. Segmentation and recognition using structure from motion point clouds. ECCV 44-57. ECCV European Conference on Computer Vision. Florence; October 12–18, 2008. .
34. Sudre CH, Li W, Vercauteren T, Ourselin S, and Cardoso MJ. Generalised dice overlap as a deep learning loss function for highly unbalanced segmentations. In: Cardoso MJ, Arbel T, Carneiro G, Syeda-Mahmood T, Tavares JMRS, Moradi M, et al., editors. *Deep Learning in Medical Image Analysis and Multimodal Learning for Clinical Decision Support*. vol. 10553 of Springer Proceedings in Computer Science. Springer; 2017. p. 240–248.
35. Kae A, Sohn K, Lee H, and Learned-Miller E. Augmenting CRFs with Boltzmann machine shape priors for image labeling. ICCV 2019-2026. ICCV IEEE International Conference on Computer Vision. Sydney; December 1–8, 2013. .
36. Borza D, Ileni T, and Darabant A. A deep learning approach to hair segmentation and color extraction from facial images. ACIVS 438-449. ACIVS International Conference on Advanced Concepts for Intelligent Vision Systems. Poitiers, France; September 24–27, 2008. .

37. Yang S, Luo P, Loy CC, and Tang X. From facial parts responses to face detection: A deep learning approach. ICCV 3676-3684. ICCV IEEE International Conference on Computer Vision. Santiago; December 11–18, 2015. .
38. Svanera M, Muhammad UR, Leonardi R, and Benini S. Figaro, hair detection and segmentation in the wild. ICIP 933-937. ICIP IEEE International Conference on Image Processing. Phoenix, Arizona; September 25–28, 2016. .
39. Sturges P, Alahari K, Ladicky L, and Torr PH. Combining appearance and structure from motion features for road scene understanding. BMVC 62.1-62.11. BMVC British Machine Vision Conference. London; September 7–10, 2009. .
40. Zhang K, Zhang Z, Li Z, and Qiao Y. Joint face detection and alignment using multitask cascaded convolutional networks. IEEE Signal Processing Letters. 2016;**23**(10):1499–1503. .
41. Yu C, Wang J, Peng C, Gao C, Yu G, and Sang N. Learning a discriminative feature network for semantic segmentation. CVPR 1857-1866. CVPR IEEE Conference on Computer Vision and Pattern Recognition. Salt Lake City; June 19–21, 2018. .
42. Badrinarayanan V, Kendall A, and Cipolla R. Segnet: A deep convolutional encoder-decoder architecture for image segmentation. IEEE Transactions on Pattern Analysis and Machine Intelligence. 2017;**39**(12):2481–2495. .
43. Li H, Xiong P, Fan H, and Sun J. Dfanet: Deep feature aggregation for real-time semantic segmentation. CVPR 9522-9531. CVPR IEEE Conference on Computer Vision and Pattern Recognition. Los Angeles; June 16–20, 2019. .

TABLE 1 HLNet consists of an asymmetric encoder and decoder. The whole network is mainly composed of standard convolution (Conv2D), deep separable convolution (DwConv2D), inverted residual bottleneck blocks, upsampling (UpSample2D) module and specially designed modules.

Satge	Type	Output Size
Encoder	-	$224 \times 224 \times 3$
	Conv2D	$112 \times 112 \times 32$
	DwConv2D	$56 \times 56 \times 64$
	DwConv2D	$28 \times 28 \times 64$
	InteractionModule	$28 \times 28 \times 64$
	FFM ²⁵	$28 \times 28 \times 64$
	DilatedGroup	$28 \times 28 \times 32$
Decoder	UpSample2D	$224 \times 224 \times 32$
	Conv2D	$224 \times 224 \times 3$
	SoftMax	$224 \times 224 \times 3$

How to cite this article: L. Luo, D. Xue, X. Feng, Y. Yu, and P. Wang (2019), Real-time Segmentation and Facial Skin Tones Grading, *Computer Animation & Virtual Worlds*, 2019;12:1–6.

TABLE 2 Segmentation performance of LFW, CelebA and Figaro1k dataset. Comparative analysis shows that our network can still achieve wonderful results when the parameter quantity is much smaller than the other two, in some metrics, even exceed the cumbersome VGG² network. All values are in %.

	LFW			CelebA			Figaro1k		
	VGG	U-Net	HLNet	VGG	U-Net	HLNet	VGG	U-Net	HLNet
mIoU	87.09	83.46	88.03	92.03	88.56	91.90	77.79	77.75	78.39
fwIoU	94.67	92.75	94.26	94.42	91.79	93.65	82.66	83.01	83.12
pixelAcc	97.01	95.83	96.01	97.06	95.54	96.78	90.15	90.28	90.73
mPixelAcc	91.81	88.84	91.26	95.77	93.61	95.53	84.75	84.72	84.93

TABLE 3 The effect of our proposed InteractionModule (IM) and DilatedGroup (DG) which is evaluated on Figaro1k testset.

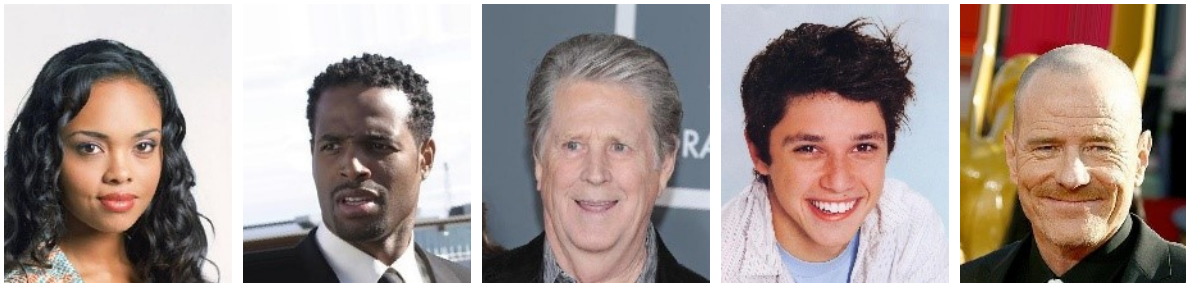
Method		mIoU
IM	DG	
-	-	74.13
-	✓	75.67
✓	-	77.32
✓	✓	78.39

TABLE 4 Results on CamVid test dataset. ‘-’ indicates that the corresponding result is not provided by the methods.

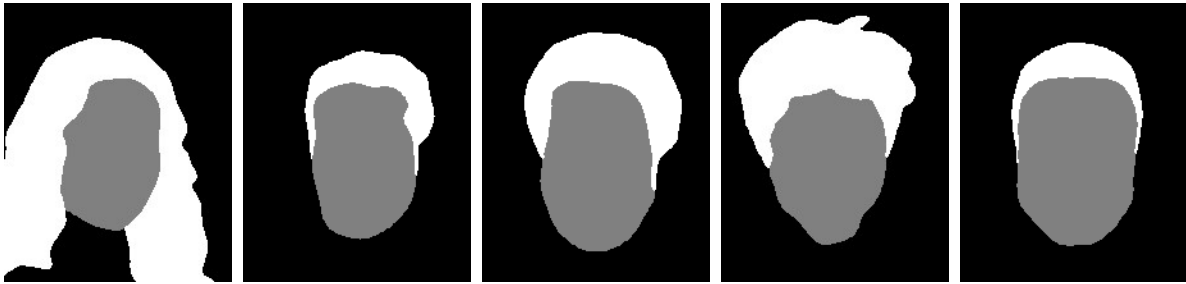
Model	Time(ms)	mIoU(%)
DPN ⁴¹	830	60.1
SegNet ⁴²	217	46.4
ICNet ¹¹	36	67.1
ENet ¹⁰	-	51.3
BiSeNet ²⁵	-	68.7
DFANet ⁴³	6	59.3
HLNet (ours)	5.3	56.3

TABLE 5 Classification accuracy of different methods in different color spaces.

	RGB	HSV	YCrCb
Histogram (8 bins)	75%	78%	73%
Histogram with PCA (256 bins)	77%	-	-
Color Moment	73%	77%	80%



(a) RGB image



(b) Ground truth



(c) Hair output



(d) Guided output



(e) Hair dyeing

FIGURE 5 Samples of hair segmentations. From top to the bottom: RGB image, Ground truth, Hair output, Guided output and Hair dyeing. The last column gives the wrong case, which also plagues the human marker.

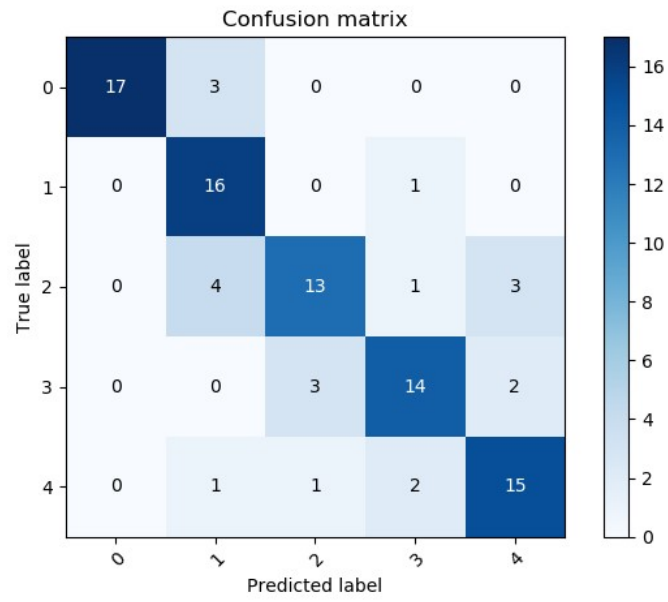


FIGURE 6 Multi-classification confusion matrix.